



# USE OF UNMANNED AERIAL VEHICLES (UAVs) TO CREATE DIGITAL OUTCROP MODELS: AN EXAMPLE FROM THE CRETACEOUS COW CREEK FORMATION, CENTRAL TEXAS

Chris Zahm<sup>1</sup>, Josh Lambert<sup>1</sup>, and Charlie Kerans<sup>2</sup>

<sup>1</sup>*Bureau of Economic Geology, Jackson School of Geosciences, University of Texas at Austin,  
University Station, Box X, Austin, Texas 78713–8924, U.S.A.*

<sup>2</sup>*Department of Geological Sciences, University of Texas at Austin,  
1 University Station C1100, Austin, Texas 78712, U.S.A.*

## ABSTRACT

The use of unmanned aerial vehicles (UAVs) has increased in popularity among field geologists as a method of collecting quantified field data. Digital photographs were collected using a UAV and a 12 megapixel camera. The methods and workflow utilized to acquire, process and construct a high-resolution 3D point cloud (i.e., latitude, longitude, and elevation) of the outcrop exposure, including a full-color (RGB) for each point, is discussed. From the point cloud, a digital outcrop model (DOM) was developed which enables analysis of bedform geometry of well-preserved beach crest and foreshore clinothems of mixed siliciclastic and carbonate grainstones within the Cretaceous Cow Creek Formation located in Central Texas. The UAV-acquired DOM analyses are compared to field measured strike and dips of the bedforms reported by other workers at the same locality and were within tolerance, but provided continuous measurements along with detailed spatial measurements of the size and shape using the inexpensive and easily created digital outcrop model.

## INTRODUCTION

Digital outcrop models (DOM), including the development of 3D models or point clouds (i.e., latitude, longitude, and elevation), on a high-density outcrop exposure have been valuable tools for quantifying the spatial relationships of geologic features in outcrop analogs for more than three decades (Deuholm, 1992; Arnot et al., 1997; Bellian et al., 2005). The term 3D model is the mathematical representation of a 3D surface or object where individual points are georeferenced and have a unique X, Y, and Z position and can be rendered or visualized within specialized software. The evolution from global positioning system (GPS) to real-time kinematic GPS (RTK–GPS) and into terrestrial light detection and ranging (LiDAR) enabled users to generate 3D models that could be interrogated for quantified geologic analysis (Hodgetts et al., 2004; Pringle et al., 2004; Bellian et al., 2005). The increased usage of digital photogrammetry software enables users to deliver comparable 3D models at a fraction of the effort and cost compared to a LiDAR survey (McCaffrey et al., 2005). Furthermore, the rise of unmanned aerial vehicles (UAVs) that

can be equipped with GPS systems and high-resolution cameras enables easily attained photogrammetry models that can be used for characterization of geologic features of interest (Starek et al., 2011; Niethammer et al., 2012; Bemis et al., 2014; Vasuki et al., 2014). Through the utilization of this digital outcrop model technology geoscientists are able to better visualize and understand stratigraphic relationships, extract geologic geometries and dimensions, and characteristics that are important to the understanding of outcrop exposures and to provide improved application to subsurface characterization for analogous reservoirs. When viewing data using 3D software or within a geographic information system (GIS) environment, data can be manipulated and interrogated beyond the fieldwork environment.

In this study, a detailed workflow for the collection and creation of 3D models of outcrop exposures using UAV-acquired images, photogrammetry and geographic information software is provided. As a demonstration of the workflow and potential usage, analysis was performed on well-exposed mixed clastic-carbonate bedforms of the lower Aptian Cow Creek Formation in Central Texas (Fig. 1) that was first described by Lozo and Stricklin (1956) and later by Owens and Kerans (2010). The techniques used in this study validate that spatial characterization of bed form geometry, the data that is essential to characterization, is done with minimal time and effort compared to previous methods of GPS or LiDAR surveys when UAV-acquired photogrammetry is utilized.

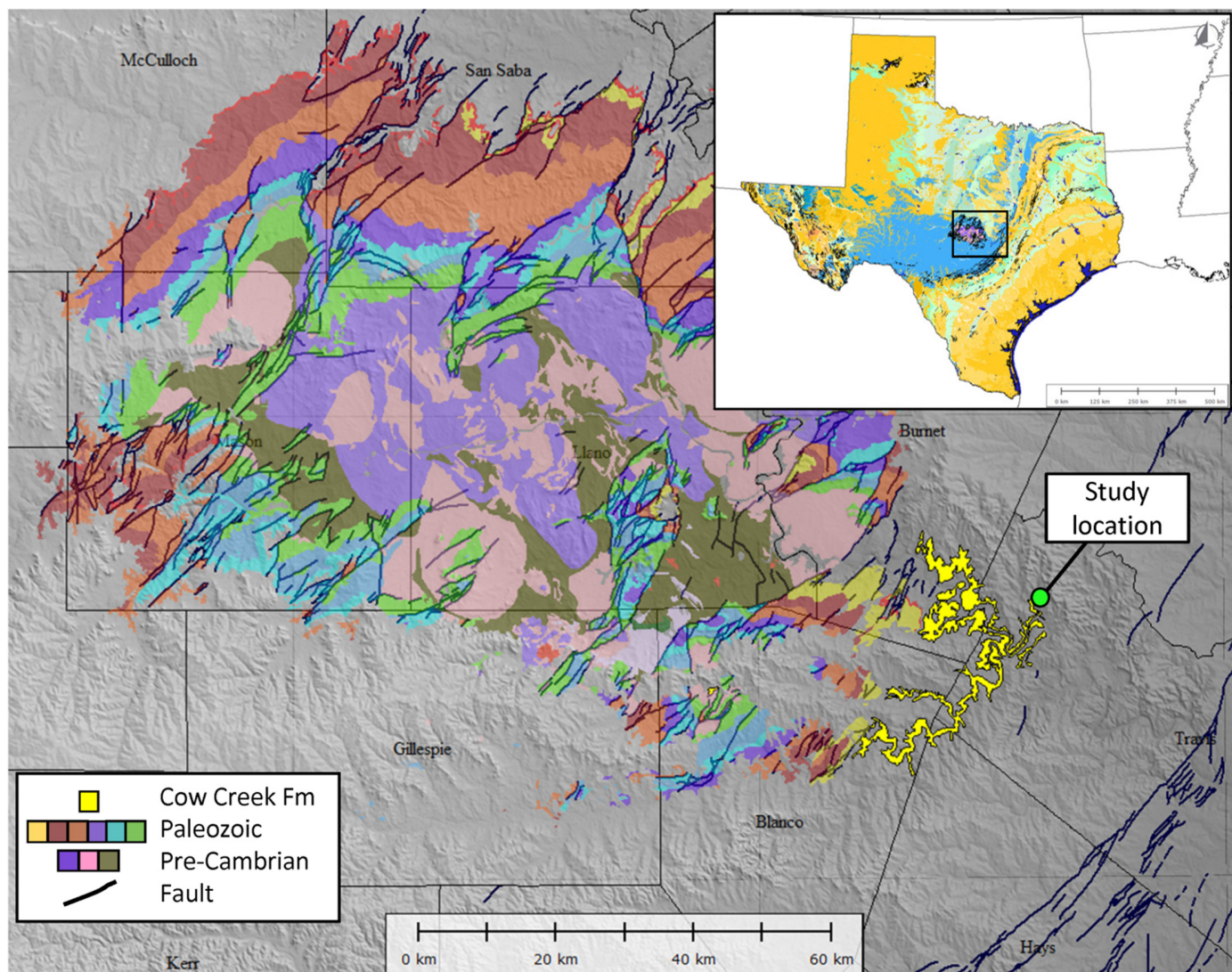


**Figure 1.** Location of study area (N 30.5141425, W 98.039329) in northwestern Travis County with the Precambrian and Paleozoic units highlighted. The yellow mapped unit is the outcrop of the Cretaceous Cow Creek Formation. Source: Texas State Geologic Map.

## STUDY AREA

In this study, an outcrop exposure of the Cretaceous Cow Creek Formation in Central Texas (latitude/longitude: 30.504226°, -98.035450°) located in the ephemeral Cow Creek north of Pace Bend State Park in western Travis County, Texas (Fig. 1) was highlighted. This classic exposure contains preserved mixed clastic-carbonate strandplain deposits with well exposed, shingled beach crest of sandy quartz oyster grainstones facies overlying trough cross bedded upper shoreface grainstones (Owens and Kerans, 2010). For details of the geology of this exposure, see Lozo and Strickland (1956), Inden (1974) and Owens and Kerans (2010). It is the geometry (i.e., bed dip and dip direction) of the shingled bed forms that are the subject of this study and the ability to remotely detect the bed forms using UAV-acquired photos.

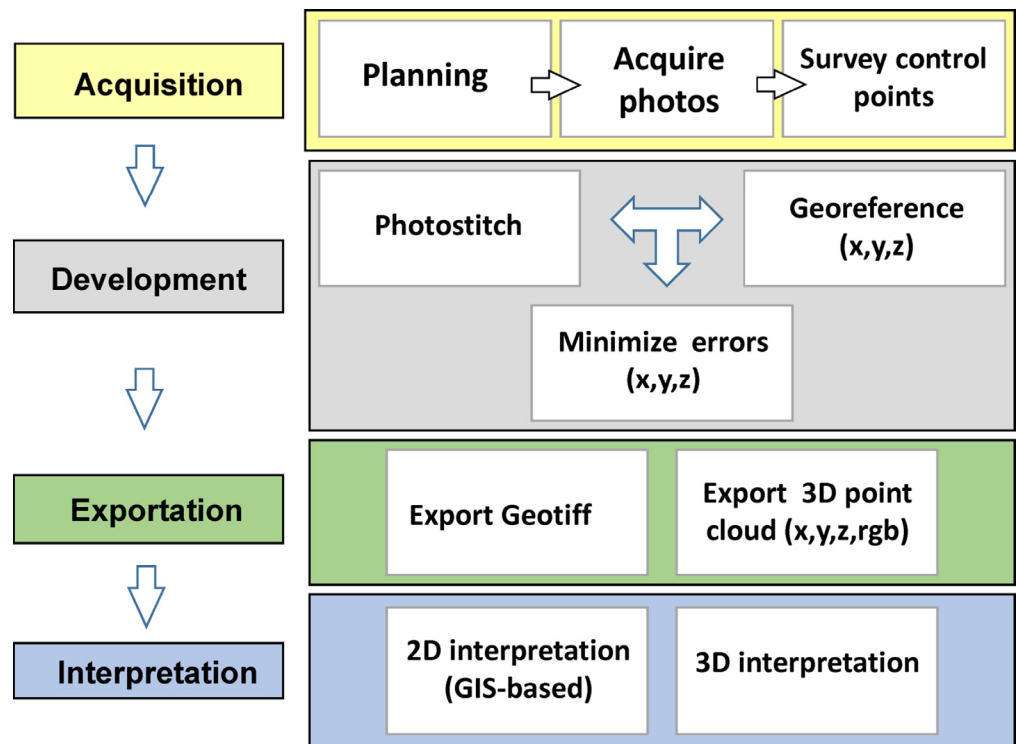
## METHODOLOGY

Photogrammetry is a well studied science that has been utilized for more than a century for creating 3D visual images using paired or multiple 2D photographs. In fact, many 7.5' quadrangle topographic maps are developed using stereoscopic photo-

graphs to map between known surveyed benchmarks. The concepts behind stereoscopic imagery have been updated and incorporated into software that enables photographs taken from different perspectives of similar objects to be combined to create 3D models. The resolution of the 3D models is a function of the pixel density of the photographs and amount of overlap between images. UAVs provide a unique way to acquire the photographs of geologic exposures where the distance from the outcrop and amount of photograph overlap can be easily controlled. Photographs acquired by the UAV for this study use gimbal-mounted cameras enabling orthogonal (e.g., straight down), lateral, or variably-angled orientations to the exposure surface making the image acquisition by UAV extremely versatile. The workflow utilized to create a high-resolution model of the outcrop exposure, including details of both the field equipment and software, are presented below. As a demonstration of the utility and accuracy of this technique, we compare detailed field measurements of bed forms by Owens and Kerans (2010) to values characterized by the UAV 3D photogrammetry model of the same exposure.

The development of 3D models from UAV-acquired photographs can be divided into four main tasks (Fig. 2): (1) planning and considerations for data usage, (2) acquisition of the data in

**Figure 2. Example work flow highlighting the acquisition through interpretation phase of UAV-acquired photogrammetry models.**



the field, (3) processing the acquired photographs and control points to create a geographically-referenced 3D model, and (4) interpretation of products generated such as GeoTIFFs and 3D point clouds (i.e., geographic position X, Y, and Z; and R, G, and B attributes). RGB is the proportion of red, green, and blue assigned for each point with a range of 0–255 for each value. The following sections describe each of the four phases.

### Planning

Prior to acquiring the photographs, consideration about the expected usage after the model is developed is important. Camera resolution in points per meter and distance from the outcrop dictate the resolution or pixel density of the developed 3D point cloud. Whereas placing the model into real world coordinates (i.e., georeferencing) determines the type of global positioning system (GPS) or survey that you will need. It has been found that having less than 1 cm per pixel allows for detailed geologic mapping of facies and 5 mm per pixel is better for fracture mapping. Given this goal, consideration of distance from outcrop and the number of photographs required to capture an area of interest is a function of the camera specifications.

Accurate placement of the 3D model into geographic information systems (GIS) packages for detailed mapping often means surveying control points with a differential GPS system. Note that the workflow and software we used created geometrically accurate models to within 15 cm of true scale over a distance of 1 km, but it is the georeferenced control points that places the 3D model in the proper global coordinates. The evolution of UAV-based photogrammetry systems continually changes and the photograph files often contain information on the GPS location of the UAV when the photograph was taken. This type of system is optimal, but if high-resolution control is desired a real-time kinematic GPS system or total station is necessary.

The final aspect of acquisition is environmental factors such as vegetation cover (e.g., trees), presence of flight obstacles (e.g., high-power lines), proximity to Federal Aviation Administration (FAA) controlled airspace, and following FAA regulations of flying below specified ceilings and keeping the UAV within site

of the controller/operator. Weather conditions are also important to the stability of the UAV as high winds (varies by unit but the recommended specification for the UAV used in this study is operating in wind speeds less than 15 mph). It has been found that developing photogrammetry models of wet or recently rain soaked outcrops is less optimal and the sun angle should be oriented for minimal shadows.

### Data Acquisition

Prior to image acquisition, twelve temporary control points or markers were placed throughout the study area (for this study white discs were used). The control points were surveyed using a differential GPS system with positional accuracy to 10 cm. The use of control point markers or targets is an easier way to post-process the data, but in cases where markers cannot be placed it is possible to survey distinct natural features as a substitute. In this case, the markers were placed prior to acquisition. Each control point was mapped using a Trimble 6-Hz receiver with data collected using a field PC notebook running the Trimble TerraSync software. The data was post-processed in Trimble Pathfinder software by applying differential correction from local Continuously Operating Reference Stations (CORS) points. After post-processing, GPS control points were georeferenced to within 6 cm horizontal and 14 cm vertical resolution. For convenience, the GPS data was referenced to Universal Transverse Mercator (UTM) Zone 14N using the World Geodetic System 1984 (WGS84) ellipsoid.

Image acquisition was conducted at the study area with a DJI Phantom 2 Quadcopter. The quadcopter was equipped with a GoPro Hero 3 Camera (12 megapixel resolution, 4000 x 3000 pixels) in conjunction with a Zenmuse H3-3D gimbal (three axis rotation). The images were taken over the course of an hour with consistent lighting conditions to establish even shadows in the model reconstruction. The quadcopter was flown at an average altitude of 30 m and images were taken in two-second intervals during the image acquisition process with the camera in an orthogonal position in respect to the outcrop exposure. In total, 821 images were taken during the acquisition process with a min-

imum of 60% overlap between sequential photographs. This overlap is essential in the image alignment process of the photogrammetry software package. The total study area acquired by imagery is 39,446 m<sup>2</sup>. With an input resolution of 12 megapixels, we established a final image resolution of 8.3 mm/pixels for the area of investigation (AOI).

### Processing Images and Georeferencing

During the processing phase of the workflow, all 821 images were imported into Agisoft Photoscan Professional software and examined for satisfactory quality (i.e., in focus and of proper

exposure balance and color tone). All 821 photographs were automatically aligned using over 1 million tie points that were determined by a point-matching algorithm used by the Photoscan software. After alignment, the 12 RTK-GPS control points were imported into the Agisoft workspace as known locations of high quality (accuracy within 10 cm in location and 15 cm in elevation). Because the control points were in place before the photographs were acquired, each photo where the control point appeared was tagged and georeferenced (Fig. 3). A minimum of six photographs was used for georeference for each control point with an average of 18 photographs being marked per control point resulting in a highly accurate and precise model.

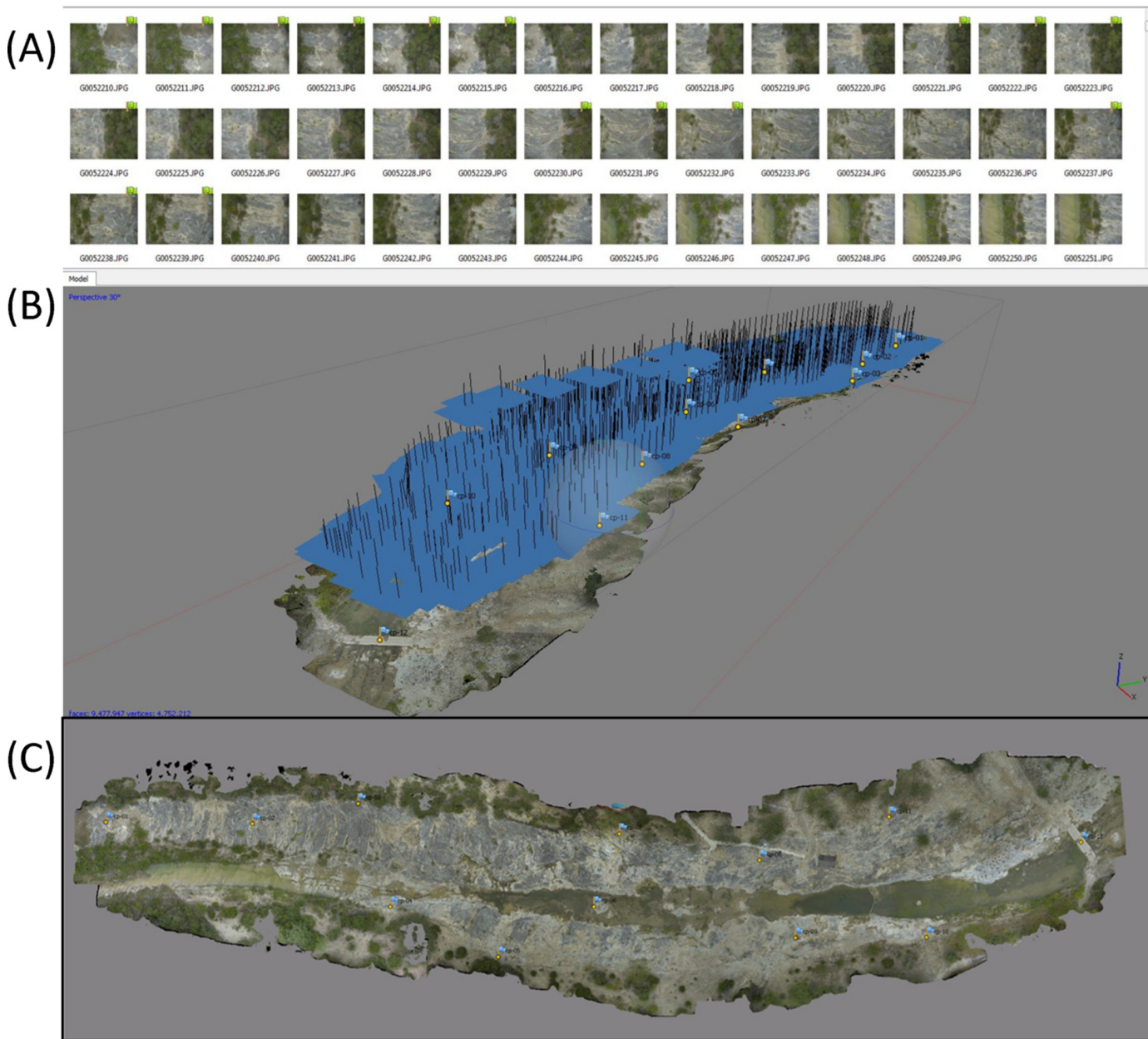


Figure 3. Construction of the photogrammetry model using UAV-acquired photographs. (A) Example of the photograph thumbnails used to stitch and align the photogrammetry model. The photographs shown are 42 of the 821 total used for the construction of the model. Flagged images denote photographs which have captured control points during acquisition. (B) Oblique view of the model showing the DEM surface with RGB values draped. The blue squares are the location where the photograph was taken (~30 m above outcrop) and the black lines are the i,j,k normals of the photograph. (C) Photomosaic GeoTIFF of the outcrop exposure with flags marking the location of the control points. This image has been dramatically reduced in size as it is 32,056 x 54,477 pixels in size and represents about 1 km<sup>2</sup> in area.

After georeferencing, a dense point cloud containing 47 million points of known X, Y, and Z locations was created from the stitched photographs. These points were then meshed into a triangular irregular network (TIN) surface containing over 9 million triangular faces. Color values, also known as RGB values, were distributed across the TIN based on the original photographs. These distributed RGB values were then transferred to the point cloud to create a 3D model with both location and color values. The 3D point cloud was exported from Agisoft Photoscan as a log American Standard Code for Information Interchange (ASCII) standard (LAS) formatted file (standard of GIS world containing X, Y, Z, and RGB data). In addition to the point cloud, an orthorectified map view image was exported from Agisoft as a georeferenced tiff (GeoTIFF) file that is 32,056 x 54,477 pixels in size (8.19 mm/pixel). Finally, a digital elevation model (DEM) was developed from the stitched images and 3D point cloud to enable calculations of dip and dip angle. The DEM for this model is 12,300 x 17,858 grid cells resulting in 3.28 cm/pixel. These products at the resolution specified ensured that analyses of the 2D and 3D data are high-resolution and sufficiently located.

### Interpretation and Analyses

The GeoTIFF and DEM file were imported into the ESRI ArcMap for analysis using the Spatial Analyst toolset. The DEM was also loaded into Quantum GIS (QGIS) and where measurements of the shape were done using the Raster Terrain Analysis toolset. Different raster outputs using the original DEM were generated to analyze different characteristics of interest within key areas of the studied exposure including shaded relief, or hill shade, which was created to assist viewing the elevation characteristics in relation to the terrain by controlling the light intensity and angle across the DEM surface (Fig. 4). Surface dip (slope) was calculated from the DEM by creating a 3 x 3 cell neighborhood around a center cell and comparing its eight neighbor cells in order to look at relative changes in Z values and to measure dip and dip direction. The dip is a continuous property that can be used to view the dip of terrain in areas where the bed forms are well preserved. Dip direction was isolated to define northern (azimuth 290–360° and 0–68°) and southern (azimuth 110–248°) facing sections.

In addition to a continuous measurement of dip using the 3D DEM, dip was analyzed along 2D topographic profiles created by the UAV–photogrammetric method to ensure that the bed forms represent the original depositional shape rather than a winnowed or eroded shape due to weathering on the outcrop surface (Fig. 5). It is impossible to know if minor weathering has occurred on the beach bed forms, but sampling each bed along a topographic profile aids in determining the degree of preservation or erosion. Bed forms expected along a strandplain beach system are expected to be asymmetric with the steep face dipping toward the predominant current direction and the lower angle limb dipping away from the current (Fig. 6). Topographic profiles were used to assess whether bed forms exhibit this typical asymmetric shape. Areas where the profile of the bed form met these criteria were used to measure the dip and dip direction compared to those measured by Owens and Kerans (2010).

## RESULTS AND DISCUSSION

The development of a high-resolution DEM of the outcrop surface enables quantification of the surface attributes such as elevation, dip, and dip direction (Fig. 7). The surface area that is characterized is also much larger compared to individual point-source measurements in the field. This level of measurement is an improved characterization overall but also provides a full statistical sampling of the attributes and has increased utility as a subsurface analog for geomodel construction in reservoirs where

similar features may exist. Furthermore, the spatial relationships such as spacing between the top of bed forms, whether the features are linear or radial, and the measured height of the bed form provides insight to the geologic conditions at time of deposition (discussed in Owens and Kerans, 2010).

One of the primary goals of this study is to demonstrate that UAV–acquired photographs can be used to develop high-resolution 3D models for interpretation of geologic features. Our choice of outcrop is based on the “ground-truth” database of bed form geometries characterized by Owens and Kerans (2010) illustrated in Fig. 3A. We have sampled the developed 3D DEM for dip and dip direction attributes to compare to strikes and dips measured by Owen and Kerans (2010). The model was queried at approximately the same locations to validate the geometries and report the measured results of this study against these previously measured as illustrated in Figure 8. Excellent conformance between the field and model-acquired measurements gives confidence that the geometry is adequately characterized by the photogrammetry method. Sources of error of bedding strike and dip are likely greater in the field measurements compared to the photogrammetry model. Small variations in the outcrop surface topology and low precision of measurement by a field compass outweigh the accuracy of the model. In addition, measurements along the topographic profile allow integration of numerous points into one measurement reducing the surface topology effect.

The use of photogrammetry for outcrop characterization is a known process as is the combination of photogrammetry from UAV–acquired photographs. Publications related to this subject have exploded in the past decade. The varied application of UAVs and photogrammetry has created a large user base, which drives innovation in all three of the main components: UAV design, camera resolution and software functionality. For this study, surveying the marker control points was the most time intensive component at approximately 2.5 hr. Acquisition of the photographs was done in less than 1 hr by an amateur pilot (i.e., the lead author) and imported into computer workstation. Mapping the control points in the photographs was approximately 1.5 hr of work. Photostitching, point cloud creation, and DEM development are automated processes that were batched and took approximately 2 hr. In total, the time from surveying to products ready for interpretation is less than one field day. It is possible to acquire photographs on a first day of field work and have high-resolution photographs or 3D models for field mapping the same day, thus enabling field mappers to use scaled, high-resolution photographs as their base maps.

The improvements to software and hardware occur at a rapid pace as well. As an example, a DJI Phantom 2 that carried a gimbaled GoPro and required surveyed ground control points to georeference the project. The total time was 9 hr of surveying and model development. Since the work for this study was completed, the DJI Phantom 3 Pro has been developed, which acquires GPS control points during the flight, has longer flying times and an integrated camera system. Using the Phantom 3, similar outcrop exposures have been mapped and worked through the described workflow of this study in 3 hr or less. It is conceived that this could be managed in a way that the UAV and workflow time may be shortened to allow the field geologist to map “real time” on images acquired minutes earlier.

## CONCLUSIONS

A workflow has been demonstrated that allows for the development of 2D and 3D digital outcrop models in less than a day for a 1 km<sup>2</sup> outcrop exposure that contains preserved bed forms within the Cretaceous Cow Creek Formation of Central Texas. An inexpensive (especially compared to LiDAR systems) UAV system was employed combined with photogrammetry software to illustrate a step function change in outcrop characterization.

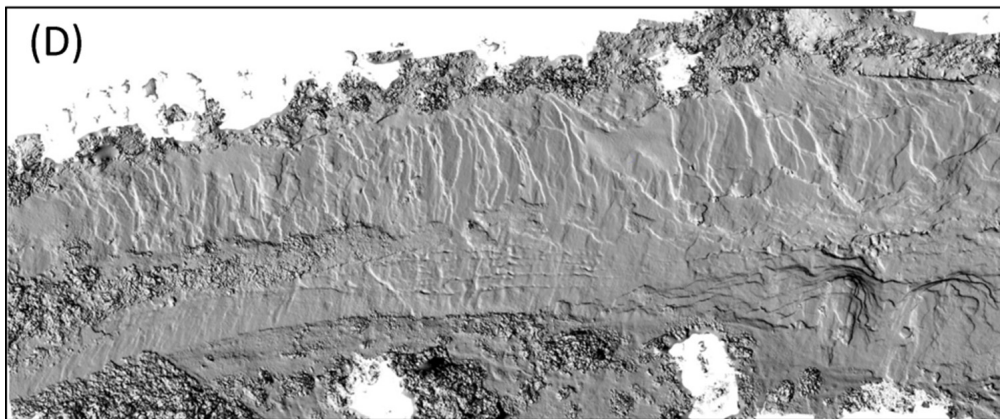
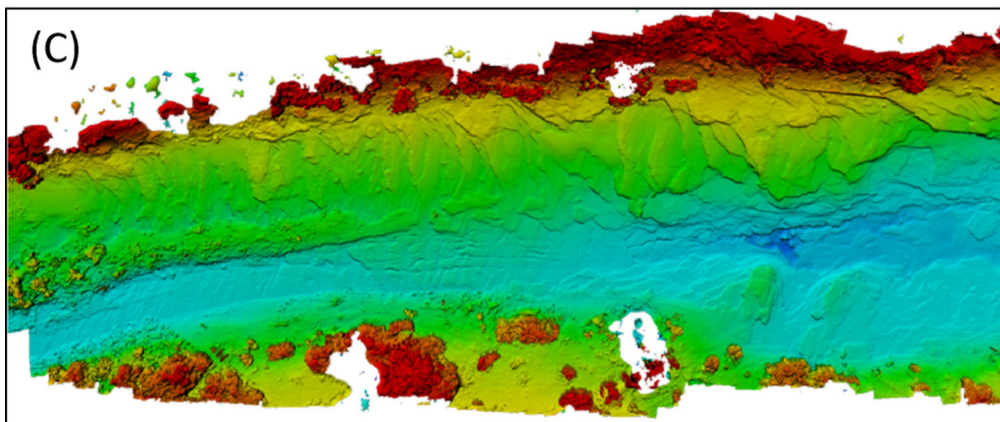
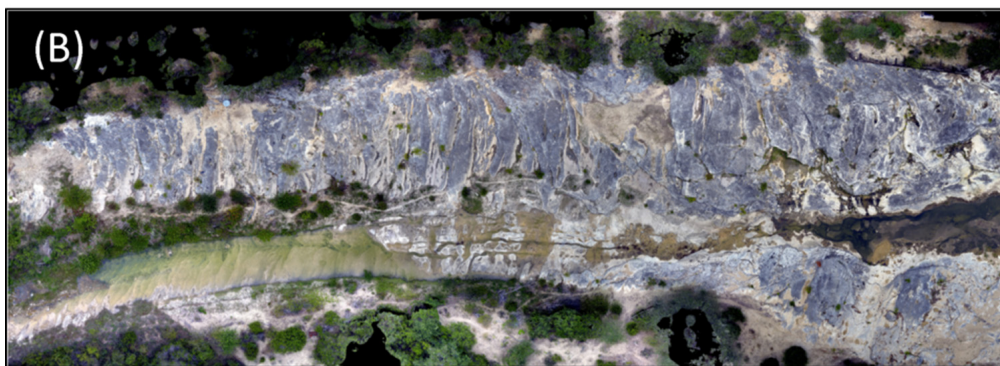
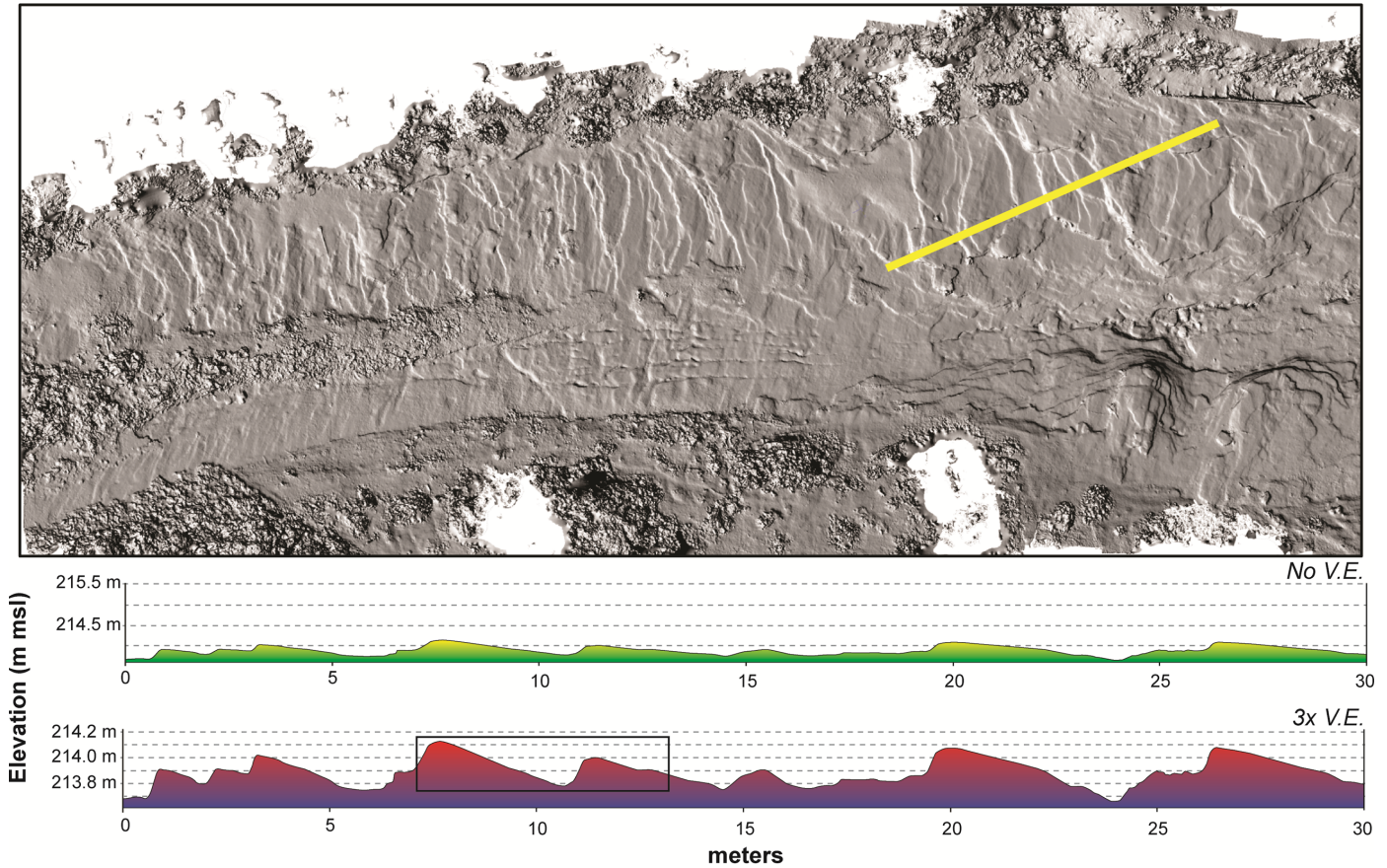
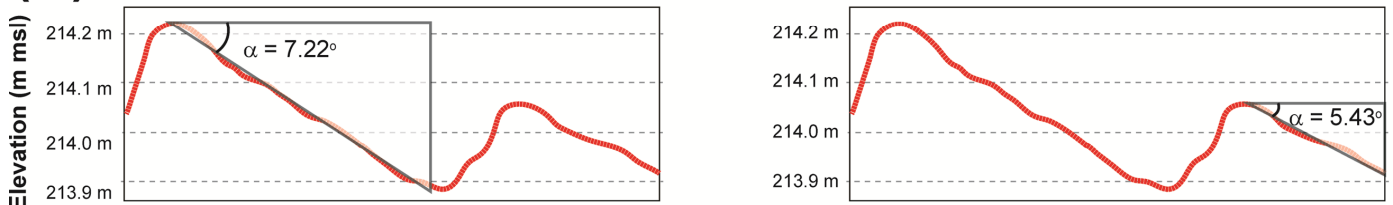


Figure 4. Map view snapshots from the outcrop study area. (A) Map of bed forms with measured strikes and dips (used with permission from Owens and Kerans (2010)); (B) high-resolution GeotIFF of the same area of investigation as (A) acquired from UAV; (C) DEM of the same exposure with red being higher elevation (>225 m above mean sea level [amsl]) than green and blue (<209 m amsl); and (D) hillshade of the DEM surface.

(A)



(B)



**Figure 5.** Topographic profiles and example of measured bedding dip from the 3D UAV-acquired point cloud model. (A) Elevation profile drawn perpendicular to dip direction (location shown with yellow line) with no vertical exaggeration (green) and 3:1 vertical exaggeration (blue). (B) Computer-measured bed dip for the boxed area in (A).

The developed model enables interrogation of high-resolution 2D and 3D models at centimeter resolution. As an example, it was demonstrated that bed forms measured from the UAV-acquired photographs are as accurate, if not more, compared to field measured strikes and dips. Based on this study and similar, it is concluded that UAV-acquired photogrammetry creates precise, accurate 3D models at a fraction of the cost of lidar and with only minor loss of data resolution.

#### ACKNOWLEDGMENTS

The authors are appreciative of the Tom Lucksinger family and the Tosalu Ranch for access to the Cow Creek exposure and to sponsors of the Reservoir Characterization Research Laboratory (RCRL), an Industrial Associates Program at the Bureau of Economic Geology, University of Texas at Austin. The authors

thank Jerome Bellian, Steve Bachtel, and Barry Katz for their reviews and improvement of this manuscript. The manuscript is published with the permission of Dr. Scott Tinker, Director of the Bureau of Economic Geology, University of Texas at Austin.

#### REFERENCES CITED

- Arnot, M. J., T. R. Good, and J. M. Lewis, 1997, Photogeological and image-analysis techniques for collection of large-scale outcrop data: *Journal of Sedimentary Research*, v. 67, p. 984–987.
- Bellian, J. A., C. Kerans, and D. C. Jennette, 2005, Digital outcrop models: Applications of terrestrial scanning lidar technology in stratigraphic modeling, *Journal of Sedimentary Research*, v. 75 no. 2, p. 166–176.
- Bemis, S. P., S. Micklethwaite, D. Turner, M. R. James, S. Akciz, S. T. Thiele, and H. A. Bangash, 2014, Ground-based and



Figure 6. Photograph from outcrop showing the asymmetric dip at top of bedform (A), followed by a constant dip plane that transitions into trough cross-stratified bedding at the base (T).

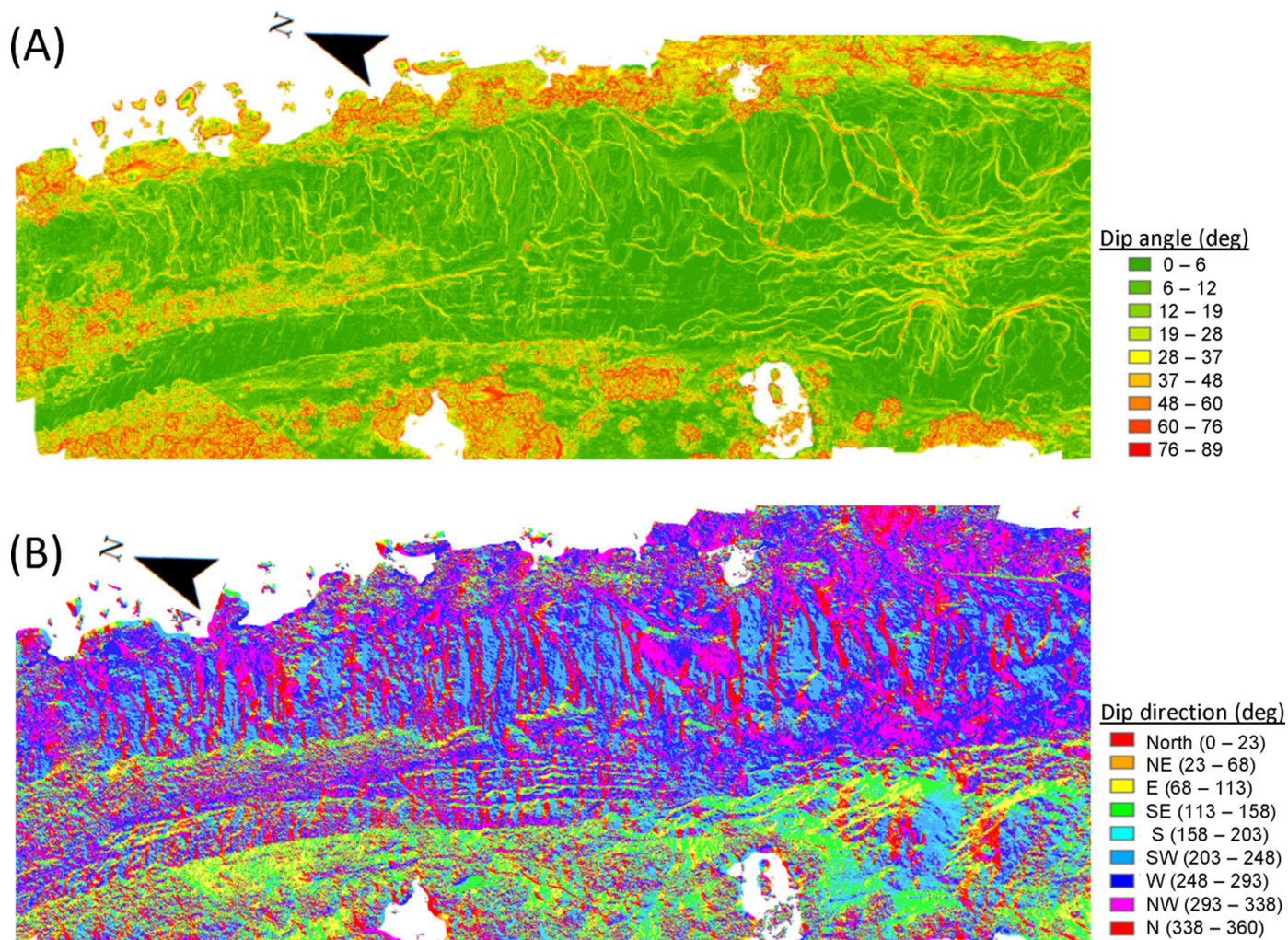
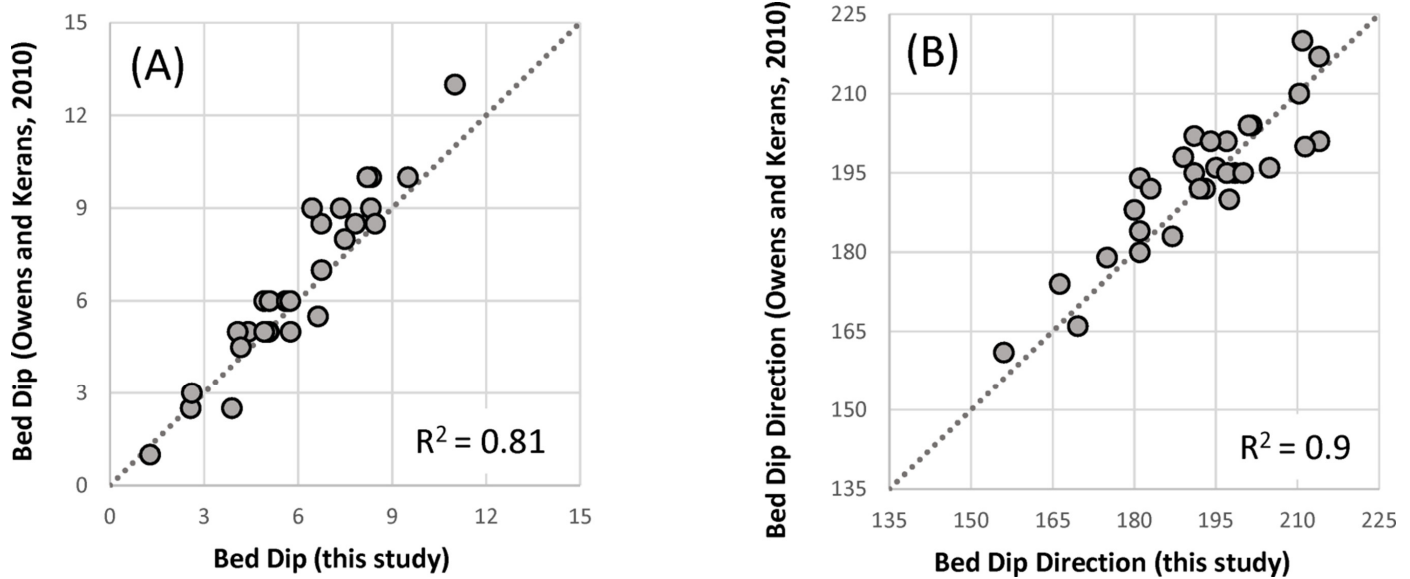


Figure 7. Map view of dip angle (A) and dip direction (B) from the outcrop exposure.



**Figure 8.** Measurements of bedding attitude from Owens and Kerans (2010) versus measurements made from 3D photogrammetry models acquired by UAV above the outcrop. (A) Bedding dip angle and (B) dip direction. Axes of both plots are degrees with true north being azimuth 0 or 360.

- UAV-based photogrammetry: A multi-scale, high-resolution mapping tool for structural geology and paleoseismology: *Journal of Structural Geology*, v. 69, p.163–178.
- Deuholm, K. S., 1990, Multi-model stereo restitution: *Photogrammetric Engineering and Remote Sensing*, v. 56, p. 239–242.
- Deuholm, K. S., and A. K. Pedersen, 1992, Geological analysis and mapping using multi-model photogrammetry: *Gronlands Geologiske Undersogelse Rapport 156*, Copenhagen, Denmark, 72 p.
- Hodgetts, D., N. J. Drinkwater, J. Hodgson, J. Kavanagh, S. S. Flint, K. J. Keogh, and J. A. Howell, 2004, 3D geological models from outcrop data using digital data collection techniques: An example from Tanqua Karoo depocentre, South Africa, in A. Curtis and R. Wood, eds., *Geological prior information: Informing science and engineering*: Geological Society of London Special Publications, v. 239, U.K., p. 57–75.
- Inden, R. F., 1974, Lithofacies and depositional model for a Trinity Cretaceous sequence, Central Texas: *Geoscience and Man*, v. 8, p. 37–52.
- Lozo, F. E., and F. L. Stricklin, 1956, Stratigraphic notes on the outcrop basal Cretaceous, Central Texas: *Gulf Coast Association Geological Society Transactions*, v. 6, p. 67–78.
- McCaffrey, K. J. W., R. R. Jones, R. E. Holdsworth, R. W. Wilson, P. Clegg, J. Imber, N. Holliman, and I. Trinks, 2005, Unlocking the spatial dimension: Digital technologies and the future of geoscience fieldwork: *Journal of the Geological Society of London*, v. 162, p. 927–938.
- Niethammer, U., M. R. James, S. Rothmund, J. Travelletti, and M. Joswig, 2012, UAV-based remote sensing of the Super-Sauze landslide: Evaluation and results: *Engineering Geology*, v. 128, p. 2–11.
- Owens, L., and C. Kerans, 2010, Revisiting the Cow Creek Limestone: Facies architecture and depositional history of a greenhouse strandplain: *Gulf Coast Association of Geological Societies Transactions*, v. 60, p. 907–915.
- Pringle, J. K., A. R. Westerman, J. D. Clark, N. J. Drinkwater, and A. R. Gardiner, 2004, 3D high-resolution digital models of outcrop analogue study sites to constrain reservoir model uncertainty: An example from Alport Castles, Derbyshire, UK: *Petroleum Geoscience*, v. 10, no. 4, p. 43–352.
- Starek, M. J., H. Mitasova, E. Hardin, K. Weaver, M. Overton, and R. S. Harmon, 2011, Modeling and analysis of landscape evolution using airborne, terrestrial, and laboratory laser scanning: *Geosphere*, v. 7, p. 1340–1356.
- Vasuki, Y., E. J. Holden, P. Kovesi, and S. Micklethwaite, 2014, Semi-automatic mapping of geological Structures using UAV-based photogrammetric data: An image analysis approach: *Computers and Geosciences*, v. 69, p. 22–32.